Article

Not peer-reviewed version

High Temperature Energy Storage Properties of $Bi_{0.5}Na_{0.5}TiO_3$-$0.06BaTiO_3$ Thin Films

Ilham Hamdi Alaoui , Nathalie Lemée , Jamal Belhadi , Francoise Le Marrec , Anna Cantaluppi , Abdelilah Lahmar *

Posted Date: 1 August 2023

doi: 10.20944/preprints202308.0006.v1

Keywords: BNT-BT thin films; thermal dielectric stability; high energy storage property

Article

High Temperature Energy Storage Properties of $Bi_{0.5}Na_{0.5}TiO_3$-0.06$BaTiO_3$ Thin Films

Ilham Hamdi Alaoui, Nathalie Lemée, Jamal Belhadi, Françoise Le Marrec, Anna Cantaluppi and Abdelilah Lahmar *

Laboratory of condensed Matter Physics, University of Picardie Jules Verne, 33 Rue Saint Leu, 80039 Amiens, France; abdel.ilah.lahmar@u-picardie.fr

* Correspondence: abdel.ilah.lahmar@u-picardie.fr; Tel.: +33-3-22-82-76-91

Abstract: $Bi_{0.5}Na_{0.5}TiO_3$-0.06$BaTiO_3$ (BNT-BT) thin films were prepared by both chemical solution (CSD) and pulsed laser deposition (PLD). The structure, dielectric, and ferroelectric properties were investigated. High stability of the dielectric permittivity ($\Delta\varepsilon/\varepsilon$(150 °C) ≤ ± 15%) over a wide temperature range from room temperature to 300 °C was obtained. Distinctly, the CSD film showed high TCC stability with variation of ± 5% up to 250°C. Furthermore, the CSD film showed an unsaturated ferroelectric hysteresis loop characteristic of the ergodic relaxor phase, however the PLD one exhibited almost saturated loop signature of the coexistence of both ergodic and non-ergodic states. The energy storage properties of the prepared films were determined using the P–E loops obtained at different temperatures. The results showed that these films exhibit stable and improved energy storage density comparable to the ceramic capacitors. Moreover, the CSD film exhibited more rigidity and better energy storage density that exceeds 1.3 J/cm^3 under low applied field of 317 KV/cm as well as interesting efficiency in a large temperature range. The obtained results are very promising for energy storage capacitors operating at high temperatures.

Keywords: BNT-BT thin films; chemical solution deposition; Pulse laser deposition; thermal dielectric stability; ferroelectric properties; high energy storage property

1. Introduction

Recently, a considerable effort is reserved for the development of a new generation of dielectric capacitors operating at high temperatures to meet the need of modern technologies [1–6].

It should be noted that the two standard capacitors COG and X7R, called type I and type II respectively, operating at high temperature no longer meet current technology requirements, which require more and more performance. Indeed, the COG, in spite of that offers a good stable capacity in an extended range of temperature from -55°C to 125°C, but it has a very low variation of the capacitance $\Delta C/C=\pm 0.54\%$ that limited its application to only in resonant circuit. Likewise, the capacity of X7R drops at high temperature, although it offers a big $\Delta C/C=\pm 15\%$ compared to the capacitor type I [7]. The ability of high charge-discharge of the dielectric capacitors makes X7R more convenient for pulsed power applications. For instance, automotive and aerospace sectors need power electronic that withstand very high temperatures. Lead- based antiferroelectric materials such $Pb(Zr,Ti)O_3$ (PZT) [8,9] and PMN-PT [10], can perfectly meet this demand, but unfortunately the lead is toxic and can harm human health and the environment [11]. Universal legislation like the European Directive 2011/65/EU 2011 has restricted the use of these harmful compounds. As an alternative, lead-free materials have attracted the attention of the scientific community with the challenge to shape a material that can meet the demands of modern technologies, more especially for pulsed power applications and in power electronic circuits [12].

Among the potential candidates, materials based on $Ba_{0.5}Na_{0.5}TiO_3$ (BNT) emerge as an ideal choice for the electrostatic energy storage capacitors. This interest is motivated by the BNT structural properties in particular the presence of a modulated phase between 200 and 300°C in bulk material, associated with the depolarization temperature (T_d) and a high Curie temperature around 325°C. In fact, BNT is among the rare perovskite that exhibits A-site disorder with the simultaneous presence

 doi:10.20944/preprints202308.0006.v1

of Bi^{3+} and Na^{+}. The local chemical order-disorder in the A-sites is reported to be responsible for this modulation. Similarly, to PMN, BNT is considered as non- ergodic relaxor materials because the applied electric field induces ferroelectricity in its matrix [13,14]. A polarization of 38 μC/cm² has been reported for NBT ceramic as well as a good piezoelectric coefficient of 73 pC/N [15,16]. In addition, the observation of a double pinched P–E hysteresis loop "Antiferroelectric- like (AFE) behavior "was found very promising for the configuration of high temperature capacitors. NBT is considered as a cubic symmetry with rhombohedral R3c and tetragonal P4bm polar nanoregions with a domination of R3c at RT. However, the BNT is prone to high conductivity and large coercive field that limit is application for energy storage capacitors. Thenceforth, the modulation of the composition in BNT matrix was adopted as an appropriate way to overcome to these drawbacks. Zhenhao et al. reported in the (1-x) NBT-x$BaSnO_3$ system low temperature thermal evolution of R3c and P4bm polar nano-regions that promote relaxation behavior and lead to a slim P-E hysteresis loop [17]. Further, Verma et al. on studying the 0.90$(Na_{0.5}Bi_{0.5})TiO_3$–$AgNbO_3$ solid solution, showed that the system undergo a thermal stabilization of the capacity in a long temperature range compatible with X7R behavior [18]. However, more interest has been devoted to the (1-x)$(Bi_{0.5}Na_{0.5})TiO_3$-x$BaTiO_3$ system, which endorses interesting morphotropic phase boundary zone(MPB) where the functional properties seem to be interesting [19,20].

In the later years, a revival interest is devoted to improve BNT- properties for this soaring topic [5–7,21–24]. Several substitutions in both A- and/or B-sites are tried, and interesting room energy storage properties were reported for BNT-based systems. However, only a few works are interested in high temperature applications [23–29]. In our previous work, we have shown that doping BNT ceramics with rare earth elements induced a high dielectric stability with low dielectric losses as well as improved energy storage at high temperature exceeded 200°C [27–29].

For the moment, the majority of studies have been focused on ceramic capacitors and few studies concerned thin films, especially for high temperature capacitors [30,31].

In a recent study, we have demonstrated that BNT-0.06$BaTiO_3$ (BNT-BT) based thin films exhibit very interesting energy storage properties at room temperature and high electric fields that exceeded by several of magnitude those obtained for solid state ceramic capacitors [32].

In this present work, the emphasis is placed on how the preparation method of BNT-BT thin film could influence the compositional modulation near the morphotropic phase boundary (MPB), the temperature stability of the dielectric permittivity, and energy storage properties at low electric field, in order to explore their potential application in miniaturized devices operating at low voltages and high temperatures.

2. Materials and Methods

Two methods were used for the preparation of the studied BNT-BT thin films. The first one is the chemical way using Bismuth acetate (III) ($C_6H_9BiO_6$), Sodium acetate ($C_2H_3NaO_2$), Barium acetate ($Ba(C_2H_3O_2)_2$), and titanium isopropoxide ($C_{12}H_{28}O_4Ti$) as starting precursors to prepare 0.3 mol/l of the precursor solution. The First step was to dissolve Bi- Ba-, Na- acetates in acetic acid with appropriate stoichiometry. Then, Ti- isopropoxide was dissolved in 2-Methoxyethanol and stabilized with acetylacetone (AcAc). The two prepared solutions were mixed together and stirred at room temperature for 24h to yield a stable solution. The final chemical solution was deposited onto Pt/SiN substrate using spin-coating layer by layer to yield thin film fabrication. The pyrolysis of each layer was done in a hotplate at 400°C for 10 min. The crystallization of the prepared films was carried out in a tube furnace at 600 °C under an O_2 atmosphere for 30 min. The final thickness was estimated around 460 nm.

For the pulsed laser deposition (PLD) method, a 1 mol.% Manganese enriched BNT-BT target was used. The films were grown at a temperature of 600 °C, in an oxygen pressure of 0.3 mbar on (111)Pt/Ti/SiO_2/Si substrate. A 248 nm KrF excimer laser was used. The laser beam was focused on the BNT-BT target surface, at a 45° angle of incidence and the laser energy was adjusted in order to produce a fluence of 2 $J.cm^{-2}$ and the laser pulse frequency was fixed at 2 Hz.

Preprints (www.preprints.org) | NOT PEER-REVIEWED | Posted: 1 August 2023 doi:10.20944/preprints202308.0006.v1

The microstructure of the studied specimens was checked using an Environmental Quanta 200 FEG, FEI microscopy (SEM) and the phase formation was carried out with an Advance D8 diffractometer (Bruker Discover; CuKα = 1.5406 Å. Raman spectroscopy was performed in a back-scattering configuration using a micro-Raman Renishaw spectrometer under a green laser excitation of 514.5 nm. The laser power was kept below 20 mW to avoid sample heating. The dielectric and ferroelectric investigations were performed using a Solartron Impedance analyzer SI-12060 and TF Analyzer 3000, aix-ACCT, respectively. A probe system attached to a Keithley 2611A source was used to measure the leakage current properties.

3. Results and discussion

3.1. Microstructural and structural investigations

The microstructure analysis of the studied films is depicted in Figure 1. Both films were dense and crack free as it is observed from SEM images. It seems that the average grain size decreases from 0.6 µm for the film elaborated with the chemical deposition method to about 0.3 µm for the sample grown by PLD. The EDX spectra carried out on both films showed the expected starting elements Bi, Na, Ba, Ti, and O. It has to be noted that for the PLD film the Manganese element is also detected, since a Mn-enriched BNT-BT target was used for PLD film deposition.

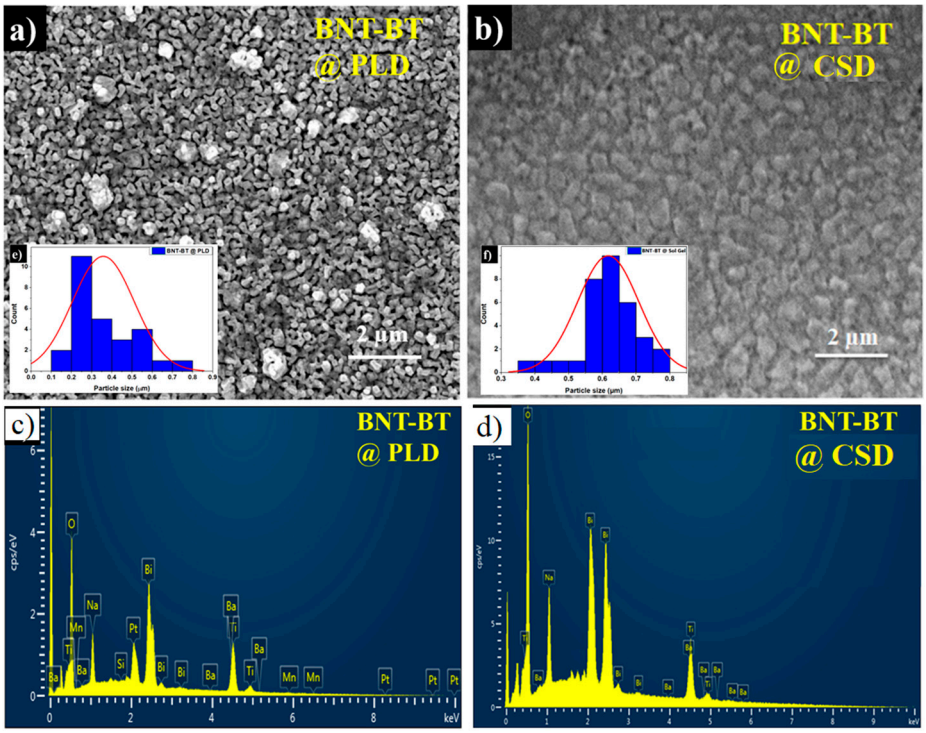

Figure 1. SEM images showing the microstructure of the investigated thin films a. BNT-BT(PLD), b. BNT-BT (CSD). The inset graph in each figure represents the average grain size distribution c. and d. EDX spectra with atomic percentage of the investigated thin films.

The average thickness of the films, determined from the cross-sectional scanning electronic microscopy measurements, was about 428 nm and 464 nm for PLD- and Sol gel respectively.

Figure 2 presents the X-ray diffractograms (XRD) of the studied samples. As reported in our previous work, the film prepared by chemical method exhibits the coexistence of the rhombohedral R3c and the tetragonal P4bm phases as expected with the bulk BNT-0.06BT composition in the vicinity of the MPB region. A more detailed discussion could be found in ref. [23]. However, the film prepared by PLD method is also polycrystalline with a dominant pseudo-cubic perovskite and a (001) preferential orientation. Noting that a small fraction of the pyrochlore $Bi_2Ti_2O_7$ secondary phase is observed, similarly to the work of Yanjiang Xie et al [33].

Preprints (www.preprints.org) | NOT PEER-REVIEWED | Posted: 1 August 2023 doi:10.20944/preprints202308.0006.v1

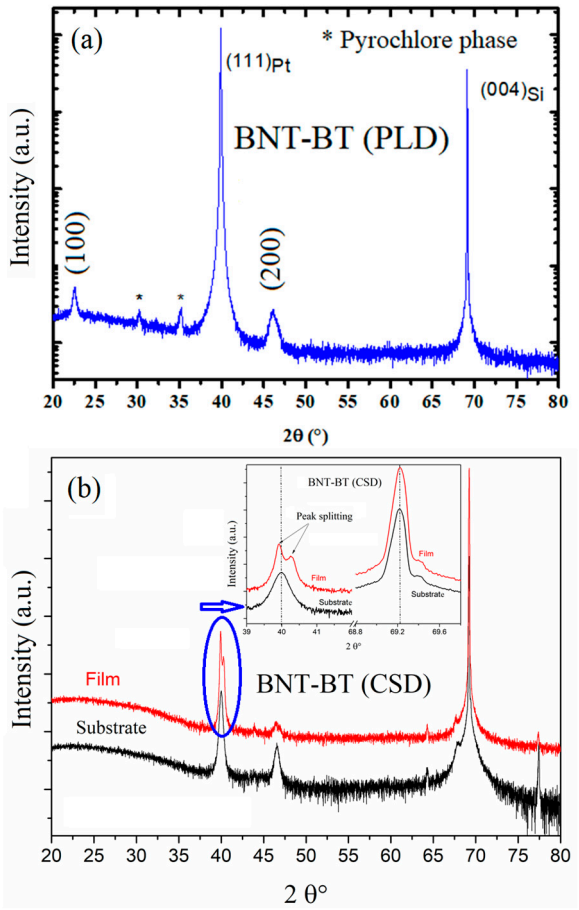

Figure 2. XRD patterns of BNT-BT thin films on Pt- substrates deposited by: (a) PLD; (b) CSD.

Complementary information about structure of the investigated film was given by Raman spectroscopy investigation. Figure 3 shows the room-temperature Raman spectra of the two studied NBT-BT thin films. The obtained Raman spectrum exhibit a relatively broad feature which are comparable to the previously reported Raman studies on NBT-BT bulk materials. This broadening could be attributed to the disorder on the A/B perovskite sites and the overlapping of Raman modes (unpolarized Raman spectra). As shown in the figure, the Raman modes in NBT-BT samples can be divided into four local vibrations involving the A-site cations displacements (modes below 100 cm^{-1}), vibrations of both A- and B-site cations (in the range 100- 200 cm^{-1}), off-center shifts of the B-site cations (100-200 cm^{-1}), and BO_6 octahedral tilts (400-1000 cm^{-1}) [34].

Preprints (www.preprints.org) | NOT PEER-REVIEWED | Posted: 1 August 2023 doi:10.20944/preprints202308.0006.v1

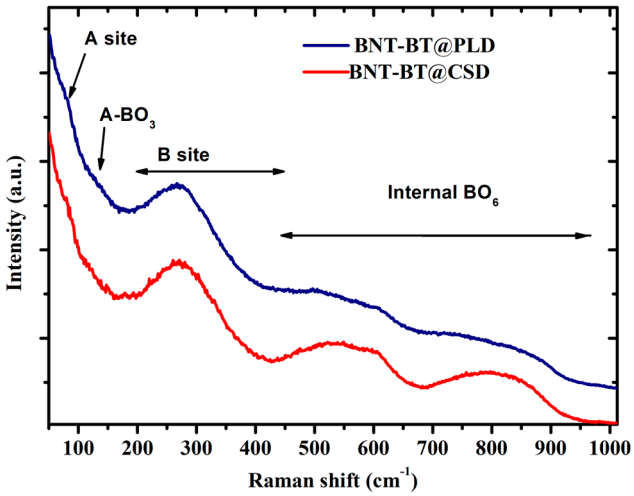

Figure 3. Room temperature Raman spectra of BNT-BT thin films deposited by PLD and CSD.

3.2. Dielectric investigation and thermal permittivity stability

Figure 4 shows the thermal evolution of the dielectric constant and of the dielectric loss for the studied BNT-BT based thin films. No clear dielectric anomalies were observed for the investigated films. In contrast, a clear dielectric loss anomaly is observed around 120°C at 10 kHz for the prepared by CSD method that correspond exactly at depolarization temperature localization. As shown in the Figure 4b, this anomaly is frequency dependent that asserts the relaxor behavior of this film [32]. Such anomaly in the dielectric loss is not detected for the film prepared by PLD method, probably because of the presence of a high leakage current and/or a rather low concentration of polar nano clusters which could not give rise to such anomaly.

It is interesting to notice that the non-observation of any dielectric anomaly until 350°C demonstrates the good dielectric temperature stability. The local stress between the substrate and film can contribute to this behavior as it is reported in the literature [35,36].

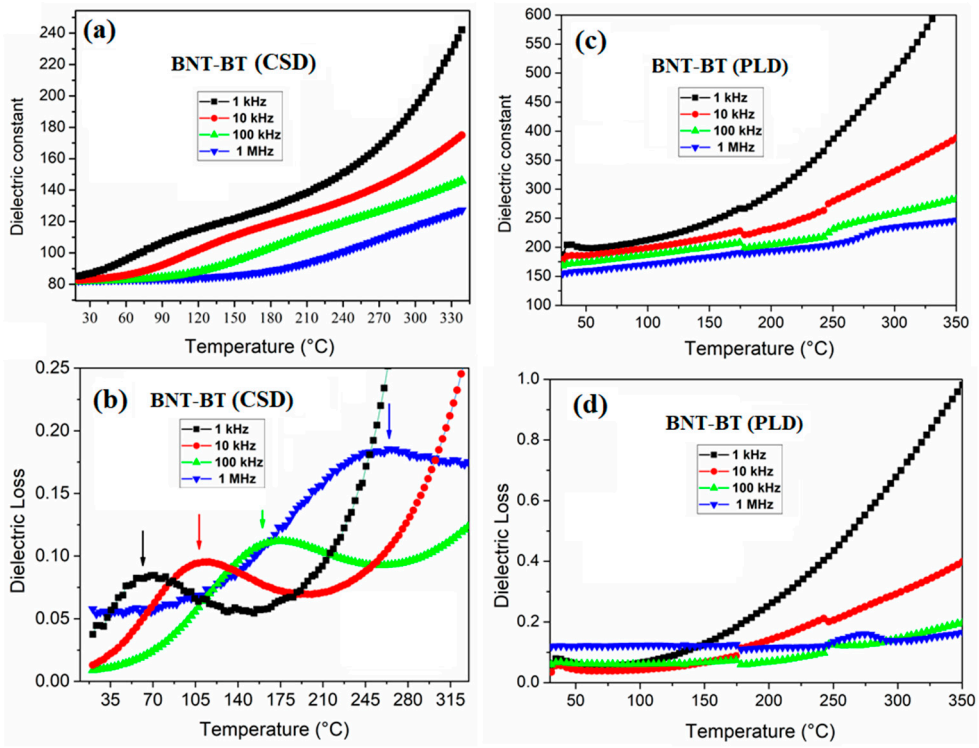

Preprints (www.preprints.org) | NOT PEER-REVIEWED | Posted: 1 August 2023 doi:10.20944/preprints202308.0006.v1

Figure 4. Thermal variation of the dielectric constant and losses: (a) and (b) CSD thin film; (c) and (d) PLD thin film.

The thermal stability of the relative permittivity of the investigated samples was evaluated by the temperature coefficient of capacitance (TCC), given by the following equation (1) [37]:

$$TCC = \frac{\Delta C}{C_{Base\,Temp}} = \frac{\Delta \varepsilon_r}{\varepsilon_{Base\,Temp}} = \frac{\varepsilon_T - \varepsilon_{Base\,Temp}}{\varepsilon_{Base\,Temp}}, \quad (1)$$

Where (ε_T) is the dielectric permittivity at a given temperature, ($\varepsilon_{BaseTemp}$) is the dielectric permittivity at the base temperature which is fixed at 150°C in this work. The value taken here for the base temperature agrees with that one used for high temperature dielectric capacitors and has been used also in several works dealing with BNT-based dielectrics materials [38,39].

The thermal evolution of TCC for both thin films is presented at some working frequencies in Figure 5. The dashed lines denote the operational range limited to ± 15% as type II capacitors. As it can be shown from the plots, all samples show good permittivity stability over a large range of temperature that exceeds 200 °C, better than the operating temperature region of X7R, especially for high temperature. Interestingly, the film prepared by CSD method shows a better TCC stability that doesn't exceed a variation of ± 15% and extended working domain exceeding 300 °C, throughout the entire frequency range under investigation. For instance, at 10 kHz, the TCC exhibits excellent stability with variation of ± 5% up to 250°C. In addition, the dielectric losses remain below 9% for the entire temperature range with a maximum obtained at the T_d anomaly.

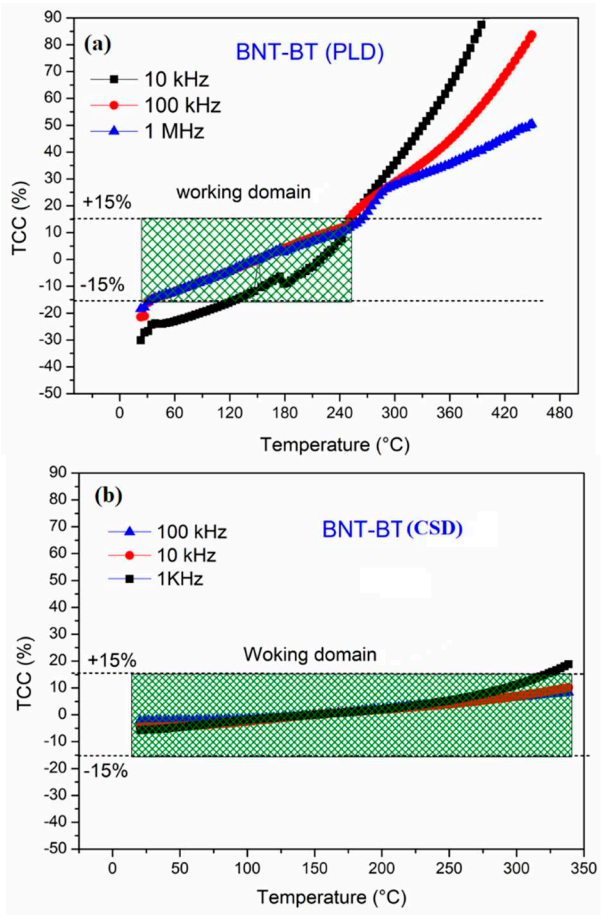

Figure 5. TCC of BNT-BT thin film prepared by (a) PLD, (b) CSD at different frequencies. The working domain for each film is highlighted by a green rectangle.

Preprints (www.preprints.org) | NOT PEER-REVIEWED | Posted: 1 August 2023 doi:10.20944/preprints202308.0006.v1

3.3. Leakage current, Ferroelectric and energy storage investigations

The current density (J) vs. electric field (E), for both films is displayed in Figure 6. The leakage current curves are fairly symmetrical about E= 0 with a high resistivity. However, film prepared by CSD method is less conductive than that one prepared by PLD as it is characterized by lower leakage currents at high electric field. The obtained results corroborate the dielectric measurement where the CSD film exhibit very low dielectric less comparing the PLD film.

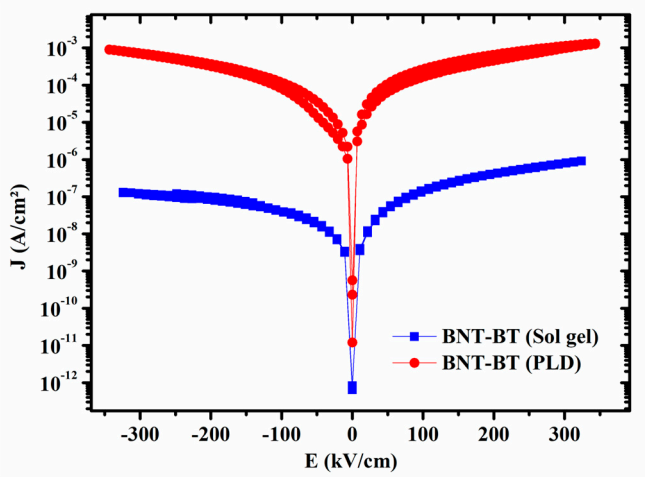

Figure 6. Room temperature J - E curve of a BNT thin films annealed under oxygen atmosphere.

Figure 7 shows the temperature dependence of P-E hysteresis loop for the investigated specimens. For the film prepared by PLD method, a clear ferroelectric hysteresis is observed at room temperature, albeit it is not well saturated because the low applied electric field. However, for the film prepared by chemical way, the obtained P-E loops have a slim shape with paraelectric-like behavior. It is worth noting that the introduction of Ba in the BNT matrix induces different relaxation states going from non-ergodic relaxor (NER) for the mother phase BNT until the paraelectric-like state. It is reported, however, that for BNT-0.06BT both the ergodic (ER) and non-ergodic states are present simultaneously because of the competition of R3c and P4mb nonpolar region, which is promising for energy storage properties. Basing on the shape of the obtained hysteresis loop, we can surmise that for the film prepared by PLD method both NER and ER coexist. Furthermore, the slim hysteresis observed for CSD film confirms the achievement of the complete ergodic relaxor phase [40].

Preprints (www.preprints.org) | NOT PEER-REVIEWED | Posted: 1 August 2023 doi:10.20944/preprints202308.0006.v1

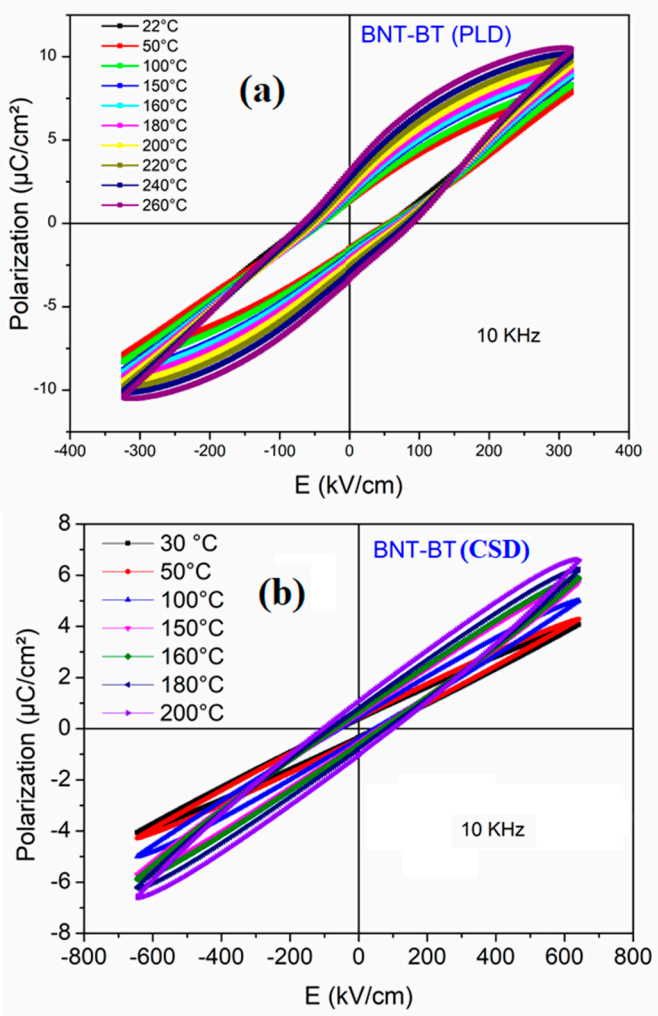

Figure 7. The evolution of the hysteresis loops vs temperature of BNT-BT (a) PLD film (b) CSD film.

Surprisingly, the increase of the temperature until 200°C doesn't seem to affect considerably the hysteresis loops as it is depicted from the temperature dependence of the ferroelectric hysteresis loop in the Figure 7. On the contrary to normal ferroelectrics, we observe in both films an increase in polarization with increasing temperature up to 200°C. This could be attributed to the presence of the ergodic and/or non-ergodic relaxor phases. Recall that it is essential to maintain high polarization at high temperatures as it plays a crucial role in achieving high energy performance in such conditions.

The energy storage properties can be calculated from the ferroelectric hysteresis loops using the integration of the polarization (P) as a function of the electric field (E):

$$W_{rec} = \int_{Pr}^{Pm} EdP, \tag{2}$$

Where (W_{rec}) is the recoverable energy density

It is interesting to mention that for obtaining a high-energy storage density both the ΔP = Pm – Pr value and the breakdown electric field should be high.

The energy loss density (W_{loss}) and the energy efficiency (η) are interesting to evaluate the discharge property of the capacitor and are calculated by using the following equations:

$$W_{loss} = \int_{0}^{Pmax} EdP - W_{rec}, \tag{3}$$

$$\eta = \frac{W_{rec}}{W_{rec}+W_{loss}} \times 100, \tag{4}$$

Preprints (www.preprints.org) | NOT PEER-REVIEWED | Posted: 1 August 2023 doi:10.20944/preprints202308.0006.v1

The thermal evolution of the recoverable energy density (W_{rec}) and energy efficiency (η) are presented in Figure 8 in the temperature range from RT to 250°C.

As it is concluded from this figure, a quasi-constant evolution of the energy storage density as a function of temperature is observed for both films. For the PLD thin film, W_{rec} is around 0.8 J cm^{-3} and the maximum of the efficiency is 55% at RT, which drops to 38% at high temperature. Interestingly, the CSD film showed improved energy storage properties with W_{rec} around 1.4 J cm^{-3} and high efficiency around 76% at RT that decreased to 40% at 250°C. Furthermore, at the temperature ≤ 180°C the efficiency still very interesting (η>70%) and remains relatively stable. The obtained values evidence better performances than some lead-free materials reported promising for high temperature application [41–43].

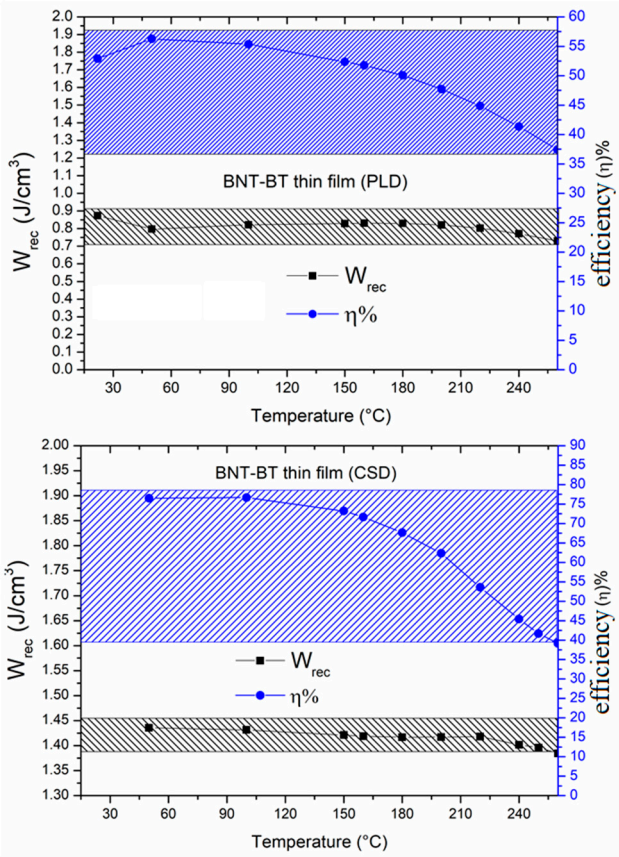

Figure 8. Recoverable energy density and efficiency of BNT-BT as a function of temperature of (a) PLD thin film; (b) CSD thin film. The hatched rectangles showed the working domain of each film.

4. Conclusions

In summary, BNT-0.06BT thin films were elaborated by both physical and chemical methods. SEM micrographs provided informations about homogeneity, density, and grain distribution in the samples. X-ray diffractograms of the investigated films confirm the formation of BNT-BT pseudo cubic perovskite and it was corroborated with Raman investigation. The temperature dielectric stability was evaluated for the investigated samples using the temperature coefficient of capacitance (TCC). Both films showed good stability of TCC in a wide temperature range exceeding 200 °C. Particularly, the film prepared by CSD method shows a better TCC stability that doesn't exceed a variation of ± 15% with and extended working domain reaching 300 °C. Besides, these films exhibit also stable energy storage properties in a large temperature range with a supremacy of the film prepared by the chemical method, whose performances are the best with a stable W_{rec}= 1.4 J cm^{-3} and high efficiency over a wide temperature range. This interesting result can be attributed to the improvement of the CSD film resistivity, as it was highlighted by the obtained low leakage current

density. This result makes the BNT-BT film prepared by the CSD, one of the best candidates for high temperature energy storage capacitor.

Author Contributions: Conceptualization, A.L. and N.L.; validation, A.L., N.L., J.B, and F.L; formal analysis, I.A and A.C.; investigation, A.C., F.L; data curation, I.A., J.B., writing—original draft preparation, A.L., I.A.; writing—review and editing, N.L, F.L, A.L, J.B; supervision, A.L. and N.L.; All authors have read and agreed to the published version of the manuscript.

Funding: This work was supported by the Region of Hauts de France (project OPPEN) and Amiens Metropole.

Data Availability Statement: Not applicable.

Acknowledgments: I. A. acknowledges financial support from the Region of Hauts de France and Amiens Metropole.

Conflicts of Interest: The authors declare no conflict of interest.

References

1. Kui Yao; Shuting Chen; Mojtaba Rahimabady; Meysam Sharifzadeh Mirshekarloo, S.Yu, F.E.H. Tay, T. Sritharan, L. Lu, "Nonlinear dielectric thin films for high-power electric storage with energy density comparable with electrochemical supercapacitors," in IEEE Transactions on Ultrasonics, Ferroelectrics, and Frequency Control, vol. 58, no. 9, pp. 1968-1974, September 2011,doi: 10.1109/TUFFC.2011.2039.
2. Zhonghua Yao, Zhe Song, Hua Hao, Zhiyong Yu, Minghe Cao, Shujun Zhang, Michael T. Lanagan, Hanxing Liu, Homogeneous/Inhomogeneous-Structured Dielectrics and their Energy-Storage Performances,Advanced Materials (2017), https://doi.org/10.1002/adma.201601727
3. Prateek, Vijay Kumar Thakur, and Raju Kumar Gupta,Recent Progress on Ferroelectric Polymer-Based Nanocomposites for High Energy Density Capacitors: Synthesis, Dielectric Properties, and Future Aspects, Chem. Rev. 2016, 116, 7, 4260–4317, https://doi.org/10.1021/acs.chemrev.5b00495
4. B. Xu, J. Íñiguez, L. Bellaiche, Designing lead-free antiferroelectrics for energy storage, Nat. Commun. 8 (2017) 15682, https://doi.org/10.1038/ncomms15682.
5. Q. Xu, M.T. Lanagan, X. Huang, J. Xie, L. Zhang, H. Hao, H. Liu, Dielectric behavior and impedance spectroscopy in lead-free BNT–BT–NBN perovskite ceramics for energy storage, Ceram. Int. 42 (2016) 9728–9736, https://doi.org/10.1016/j.ceramint.2016.03.062
6. X. Lu, J. Xu, L. Yang, C. Zhou, Y. Zhao, C. Yuan, Q. Li, G. Chen, H. Wang, Energy storage properties of (Bi0.5Na0.5)0.93Ba0.07TiO3 lead-free ceramics modified by La and Zr co-doping, J. Mater. 2 (2016) 87–93, https://doi.org/10.1016/j.jmat.2016.02.001.
7. A. Zeb, S. J. Milne, High temperature dielectric ceramics: a review of temperature-stable high-permittivity perovskites, J Mater Sci: Mater Electron (2015) 26:9243-9255, https://doi.org/10.1007/s10854-015-3707-7
8. Scott JF, Araujo CAP de (1989) Ferroelectric Memories. Science 246:1400–1405. https://doi.org/10.1126/science.246.4936.1400
9. Jaffe H (1958) Piezoelectric Ceramics. J American Ceramic Society 41:494–498. https://doi.org/10.1111/j.1151-2916.1958.tb12903.x
10. Katzke H, Dietze M, Lahmar A, et al (2011) Dielectric, ultraviolet/visible, and Raman spectroscopic investigations of the phase transition sequence in 0.71Pb(Mg1/3Nb2/3)O3-0.29PbTiO3 crystals. Phys Rev B 83:174115. https://doi.org/10.1103/PhysRevB.83.174115
11. Parliament, T.H.E.E.; Council, T.H.E.; The, O.F.; Union, E. Directive 2011/83/EU of the European Parliament and of the Council. Fundam. Texts Eur. Priv. Law 2020, 88–110, doi:10.5040/9781782258674.0031.
12. Stefanie A. Sherrill, Parag Banerjee, Gary W. Rubloff, Sang Bok Lee,High to ultra-high power electrical energy storage, Phys. Chem. Chem. Phys.,2011,13, 20714-20723, https://doi.org/10.1039/C1CP22659B
13. I. G. Siny, C.-S. Tu, and V. H. Schmidt, Critical acoustic behavior of the relaxor ferroelectric (Bi0.5Na0.5)TiO3 in the intertransition region, Phys. Rev. B 51, 5659 – Published 1 March 1995,https://doi.org/10.1103/PhysRevB.51.5659
14. Vladimir V. Shvartsman, Doru C. Lupascu, Lead-Free Relaxor Ferroelectrics, Journal of the American Ceramic Society 95 (2012)1-26, https://doi.org/10.1111/j.1551-2916.2011.04952.x
15. Suchanicz J, Ptak WS (1990) On the phase transition in Na0.5Bi0.5TiO3. Ferroelectrics Letters Section 12:71–78. https://doi.org/10.1080/07315179008201119
16. Hiruma Y, Nagata H, Takenaka T (2009) Thermal depoling process and piezoelectric properties of bismuth sodium titanate ceramics. Journal of Applied Physics 105:084112. https://doi.org/10.1063/1.3115409
17. Z. Fan, Y. Yu, J. Huang, Q. Zhang, Y. Lu, Y. He,Excellent energy storage properties over a wide temperature range under low driving electric fields in NBT-BSN lead-free relaxor ferroelectric ceramics, Ceram. Int., 47 (2021), pp. 4715-4721, 10.1016/j.ceramint.2020.10.040

18. A. Verma, A.K. Yadav, S. Kumar, V. Srihari, R. Jangir, H.K. Poswal, S. Sen,Improvement of energy storage properties with the reduction of depolarization temperature in lead-free (1 – x) Na0.5Bi0.5TiO3 - xAgTaO3 ceramics J. Appl. Phys., 125 (2019), Article 054101, 10.1063/1.5075719
19. Jamil Ur Rahman, A.l.i. Hussain, Adnan Maqbool, Gyung Hyun Ryu, Tae Kwon Song, Won-Jeong Kim, Myong Ho Kim, Field induced strain response of lead-free BaZrO3 modified Bi0.5Na0.5TiO3–BaTiO3 ceramics, J. Alloy. Compd., 593 (2014), pp. 97-102, https://doi.org/10.1016/j.jallcom.2014.01.031
20. Jeong-Ho Cho, Young-Hun Jeong, Joong-Hee Nam, Ji-Sun Yun, Yong-Joon Park, Phase transition and piezoelectric properties of lead-free (Bi1/2Na1/2)TiO3–BaTiO3 ceramics, Ceram. Int., 40 (2014), pp. 8419-8425, https://doi.org/10.1016/j.ceramint.2014.01.051
21. M. Zannen, A. Lahmar, M. Dietze, H. Khemakhem, A. Kabadou, M. Es-Souni, Structural, optical, and electrical properties of Nd-doped Na0.5Bi0.5TiO3, Mater. Chem. Phys. 134 (2–3) (2012) 829–833, https://doi.org/10.1016/j.matchemphys.2012.03.076.
22. A. Mishra, B. Majumdar, R. Ranjan, A complex lead-free (Na, Bi, Ba)(Ti, Fe)O3 single phase perovskite ceramic with a high energy-density and high dischargeefficiency for solid state capacitor applications, J. Eur. Ceram. Soc. 37 (2017) 2379–2384, https://doi.org/10.1016/j.jeurceramsoc.2017.01.036.
23. H. Yang, F. Yan, Y. Lin, T. Wang, F. Wang, High energy storage density over a broad temperature range in sodium bismuth titanate-based lead-free ceramics, Sci. Rep. 7 (2017) 8726, https://doi.org/10.1038/s41598-017-06966-7.
24. M. Zannen, J. Belhadi, M. Benyoussef, H. Khemakhem, K. Zaidat, M. El Marssi, A. Lahmar, Electrostatic energy storage in antiferroelectric like perovskite, Superlattices Microstruct. (2018) 1–6, https://doi.org/10.1016/j.spmi.2018.03.041.
25. W.P. Cao, W.L. Li, X.F. Dai, T.D. Zhang, J. Sheng, Y.F. Hou, W.D. Fei, Large electrocaloric response and high energy-storage properties over a broad temperature range in lead-free NBT-ST ceramics, J. Eur. Ceram. Soc. 36 (2016) 593–600, https://doi.org/10.1016/j.jeurceramsoc.2015.10.019.
26. W. Cao, W. Li, T. Zhang, J. Sheng, Y. Hou, Y. Feng, Y. Yu, W. Fei, High-energy storage density and efficiency of (1−x)[0.94NBT–0.06BT]–xST lead-free ceramics, Energy Technol. 3 (2015) 1198–1204, https://doi.org/10.1002/ente.201500173.
27. M. Zannen, A. Lahmar, Z. Kutnjak, J. Belhadi, H. Khemakhem, M.E.L. Marssi, Electrocaloric effect and energy storage in lead free Gd0.02Na0.5Bi0.48TiO3 ceramic, Solid State Sci. 66 (2017) 31–37, https://doi.org/10.1016/j.solidstatesciences.2017.02.007
28. Benyoussef, M.; Zannen, M.; Belhadi, J.; Manoun, B.; Kutnjak, Z.; Vengust, D.; Spreitzer, M.; El Marssi, M.; Lahmar, A. Structural, Dielectric, and Ferroelectric Properties of Na0.5(Bi1-XNdx)0.5TiO3 Ceramics for Energy Storage and Electrocaloric Applications. Ceram. Int. 2021, 47, 26539–26551, doi: 10.1016/j.ceramint.2021.06.068.
29. Benyoussef, M.; Zannen, M.; Belhadi, J.; Manoun, B.; Kutnjak, Z.; Vengust, D.; Spreitzer, M.; El Marssi, M.; Lahmar, A. Structural, Dielectric, and Ferroelectric Properties of Na0.5(Bi1-XNdx)0.5TiO3 Ceramics for Energy Storage and Electrocaloric Applications. Ceram. Int. 2021, 47, 26539–26551, doi: https://doi.org/10.1016/j.ceramint.2021.06.068.
30. Tiandong Zhang, Weili Li, Yafei Hou, Yang Yu, Ruixuan Song, Wenping Cao, Weidong Fei, High-energy storage density and excellent temperature stability in antiferroelectric/ferroelectric bilayer thin films Am Ceram Soc. 2017;00:1–8. https://doi.org/10.1111/jace.148768
31. Muying Wu, Shihui Yu, Xiaohu Wang, Lingxia Li,Ultra-high energy storage density and ultra-wide operating temperature range in Bi2Zn2/3Nb4/3O7 thin film as a novel lead-free capacitor Journal of Power Sources Volume 497, 15 June 2021, 229879 1.
32. Ilham Hamdi Alaoui , Mebarki Moussa, Nathalie Lemée, Françoise Le Marrec, Anna Cantaluppi, Delphine Favry and Abdelilah Lahmar, Influence of the Addition of Rare Earth Elements on the Energy Storage and Optical Properties of Bi0.5Na0.5TiO3–0.06BaTiO3 Polycrystalline Thin Films, Materials 2023, 16, 2197. https://doi.org/10.3390/ma16062197
33. G. de la Flor, T. Malcherek, S. Gorfman, B. Mihailova, Structural transformations in (1-x)Na0.5Bi0.5TiO3-xBaTiO3 single crystalsstudied by Raman spectroscopy, PHYSICAL REVIEW B 96, 214102 (2017), DOI: 10.1103/PhysRevB.96.214102
34. Yanjiang Xie, Hua Hao, Juan Xie, Shuo Zhang a, Minghe Cao, Zhonghua Yao, Hanxing Liu Ceramics International Volume 47, Issue 16, 15 August 2021, Pages 23259-23266, https://doi.org/10.1016/j.ceramint.2021.05.038
35. M.K. Bhattarai, K.K. Mishraa, A.A. Instana, B.P. Bastakoti, R.S. Katiyar, Enhanced energy storage density in Sc3+ substituted Pb(Zr0.53Ti0.47)O3 nanoscale films by pulse laser deposition technique, Appl. Surf. Sci., 490 (2019), pp. 451-459
36. Z. Zhao, V. Buscaglia, M. Viviani, M. Nygren, M. Johnsson, P. Nanni, Grain-size effects on the ferroelectric behavior of dense nanocrystalline BaTiO3 ceramics, Phys. Rev., B 70 (2004), p. 24107

37. Yang H, Yan F, Lin Y, Wang T, Wang F (2017) High energy storage density over a broad temperature range in sodium bismuth titanate-based lead-free ceramics. Scientific reports 7:1-12. https://doi.org/10.1038/s41598-017-06966-7
38. Acosta M, Zang J, Jo W, Rödel J (2012) High-temperature dielectrics in CaZrO3-modified Bi1/2Na1/2TiO3-based lead-free ceramics. J. of the European Ceramic Society 32:4327-4334. https://doi.org/10.1016/j.jeurceramsoc.2012.06.011
39. Park SE, Chung SJ, Kim IT, Hong KS (1994) Nonstoichiometry and the long-range cation ordering in crystals of (Na1/2Bi1/2)TiO3. Journal of the American Ceramic Society 77:2641-2647.https://doi.org/10.1111/j.1151-2916.1994.tb04655.x
40. Benyoussef, M.; Zannen, M.; Belhadi, J.; Manoun, B.; Kutnjak, Z.; Vengust, D.; Spreitzer, M.; El Marssi, M.; Lahmar, A. Structural, dielectric, and ferroelectric properties of Na0.5(Bi1-xNdx)0.5TiO3 ceramics for energy storage and electrocaloric applications. Ceram. Int. 2021, 47, 26539–26551, doi: 10.1016/j.ceramint.2021.06.068
41. A. Mishra, B. Majumdar, R. Ranjan, A complex lead-free (Na, Bi, Ba)(Ti, Fe)O3, single phase perovskite ceramic with a high energy-density and high discharge efficiency for solid state capacitor applications, J. Eur. Ceram. Soc. 37 (2017) ; 2379–2384, https://doi.org/10.1016/j.jeurceramsoc.2017.01.036.
42. W.P. Cao, W.L. Li, X.F. Dai, T.D. Zhang, J. Sheng, Y.F. Hou, W.D. Fei, Large electrocaloric response and high energy-storage properties over a broad temperature range in lead-free NBT-ST ceramics, J. Eur. Ceram. Soc. 36 (2016) 593–600, https://doi.org/10.1016/j.jeurceramsoc.2015.10.019
43. X. Liu, H. Du, X. Liu, J. Shi, H. Fan, Energy storage properties of BiTi0.5Zn0.5O3-Bi0.5Na0.5TiO3-BaTiO3 relaxor ferroelectrics, Ceram. Int. 42 (2016) 17876–17879, https://doi.org/10.1016/j.ceramint.2016.08.087